Turbulent Boundary-Layer Separation due to a Forward-Facing Step

K.R. Czarnecki* and Mary W. Jackson*
NASA Langley Research Center, Hampton, Va.

Pressure distribution tests were made at Mach numbers of 1.61 and 2.20, over a step-height range from 0.005 to 2.54 cm, and an effective length Reynolds number range from about 8 to 150 million. The results were compared with some obtained at higher Mach numbers at approximately comparable boundary-layer conditions. The comparison showed several unexplainable anomalies, and pointed up the lack of boundary-layer information necessary for a proper analysis. An analysis of the data indicates the existence of a transverse vortex in the separated-flow region which weakens with increases in Reynolds and Mach number and significantly affects the pressure distributions.

Nomenclature

$C_{N_{q_\infty,k}}$ = normal-force coefficient, $N/q_\infty,k$
a_∞ = freestream speed of sound
h = height of opening in flattened surface orifice
k = step height
M_∞ = freestream Mach number
N = normal force, positive upward
p = wall static pressure
p_{sep} = static pressure at separation point
p_∞ = freestream static pressure
q_∞ = freestream dynamic pressure
R_{δ^*} = Reynolds number, $\rho_\infty u_\infty \delta^*/u_\infty$
u_∞ = freestream velocity
x = distance from front face of step in upstream direction
x_{sep} = distance to separation point
δ = total boundary-layer thickness
δ^* = boundary-layer displacement thickness
θ = boundary-layer momentum thickness
μ_∞ = freestream viscosity coefficient
ρ_∞ = freestream density

Introduction

THE experimental study at supersonic speeds of turbulent boundary-layer separation due to a forward-facing step has many useful applications. At low ratios of step-height to boundary-layer thickness the data are helpful in predicting surface roughness effects on aircraft drag and performance; at larger ratios the results can be used to predict the effectiveness of spoilers and deceleration devices. For the full range of ratios, the data are crucial to the development of reliable empirical and theoretical solutions to the problem of estimating the shock-boundary-layer flow interactions. Unfortunately, most of the available data have been obtained on small models at low Reynolds numbers, and much of the detail needed to gain an understanding of the basic flow phenomena has been lost. Furthermore, past attempts at correlating the results have not enhanced significantly our understanding of the detailed flow phenomena nor have they isolated all the important nondimensional parameters. The result has been an obscuration of some significant trends and flow details. For these reasons, an experimental investigation was conducted utilizing a relatively large-scale step model mounted on the sidewall of the Langley 4-by 4-ft supersonic pressure tunnel, where the boundary-layer thickness varies from about 4 to 7.5 cm. Tests were carried out at Mach numbers of 1.61 and 2.20 over a unit Reynolds number range from 2.20 to 26.50 million, and some comparisons are made with higher Mach number results from other sources which have approximately comparable boundary-layer conditions.

Presented as Paper 74-581 at the AIAA 7th Fluid and Plasma Dynamics Conference, Palo Alto, Calif., June 17-19, 1974; submitted June 26, 1974; revision received June 20, 1975.

Index categories: Boundary Layers and Convection Heat Transfer-Turbulent; Jets, Wakes, and Viscid-Inviscid Flow Interactions; Supersonic and Hypersonic Flow.

*Aero-Space Technologist, Subsonic-Transonic Aerodynamics Division.

Model and Tests

Figure 1 shows a schematic of the step model mounted in the sidewall of the Langley 4-by 4-ft supersonic pressure tunnel. The essential feature of the design was that the movable block was made as large as possible yet still allowed very accurate positioning and alinement while the tunnel was in operation. The figure also illustrates the method used to install surface pressure tubes to measure in steep pressure gradients so that significant details will not be lost. All orifices were connected to two manometer boards, one of which was filled with a light liquid (alkazene) to insure large deflections for small pressures and the other was filled with a heavy one (mercury) to register the higher pressures. Extreme care was taken that no lags were in existence when the boards were photographed. Also, the tunnel test section was calibrated for changes in freestream Mach number resulting from changes in stagnation pressure. These procedures allow the pressure coefficients or pressure ratios to be determined to one order of accuracy higher than in usual techniques. (See Ref. 1, for example, where similar care was exercised.) Previous calibrations have indicated that the variations in spanwise flow outside the boundary layer were negligible.

Tests were made at nominal Mach numbers of 1.61 and 2.20, step heights from 0.005 to 2.54 cm, and a unit Reynolds number range from 2.20 to 26.50 million/m. The effective flat-plate length Reynolds number range varied from 8 to 150

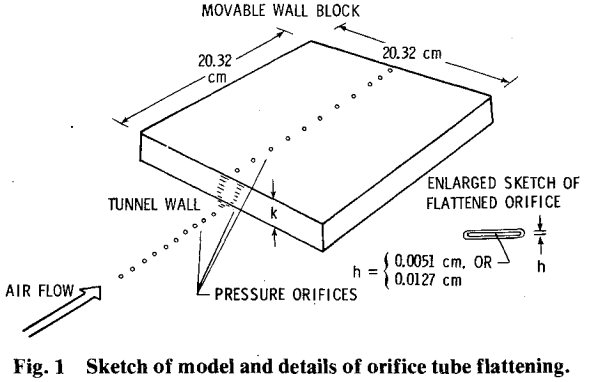

Fig. 1 Sketch of model and details of orifice tube flattening.

Table 1 Test unit Reynolds number and boundary-layer displacement thicknesses

$M_\infty = 1.61$		$M_\infty = 2.20$	
Unit Reynolds number, 1/m	δ^*,cm	Unit Reynolds number, 1/m	δ^*,cm
2.78×10^6	1.142	2.20×10^6	1.844
4.62×10^6	1.123	3.67×10^6	1.669
9.15×10^6	1.099	7.25×10^6	1.460
13.71×10^6	1.092	10.87×10^6	1.350
18.86×10^6	1.036	14.43×10^6	1.271
22.57×10^6	0.998	17.72×10^6	1.219
26.50×10^6	0.960	20.82×10^6	1.178

million. Table 1 relates the test unit Reynolds numbers and boundary-layer displacement thicknesses. The ratio of step height to boundary-layer total thickness varied from nearly 0 to approximately 0.3.

Boundary-layer characteristics required for the analysis of the measured pressure distributions were interpolated from Ref. 2 for the station corresponding to the front face of the step. As indicated in Ref. 2, the tunnel-wall boundary layer is not fully two dimensional. Consequently, tests were made with model extensions to determine aspect-ratio effects due to both the three-dimensionality of the boundary layer and step end effects. Unfortunately, a pressure-relief diaphragm began leaking air with a high moisture content into the tunnel during this period, and the desired tunnel conditions could not be maintained. When this set of results was reduced some time later, it was found that the quality of the flow in the test section had seriously deteriorated, and that reference conditions without model extensions had not been reproduced satisfactorily. An analysis of the defective data indicated that some effect due to the spanwise nonuniformity of the boundary layer did exist but that the effects were small. A study was also made of available data for step end effects, and some pressure distribution results obtained ahead of a spoiler mounted on a sharp-edged flat plate[3] are presented in Fig. 2. The tests were performed in the same wind tunnel and at the same Mach number as the lower Mach number of the present tests. Figure 2 indicates that for an aspect ratio of 12 a considerable portion of the flow over the central part of the spoiler is essentially two-dimensional. Furthermore, analysis of the results of Ref. 3 indicates that at the center line of the spoiler, which corresponds to the location of the measurement station in the present investigation, there are no changes in the pressure distributions as the aspect ratio is reduced from nearly 16, the maximum for the spoiler, to 12, the minimum. The data also indicate that if the aspect ratio is decreased further the departure from two-dimensionality at the model center line will be very gradual so that at an aspect ratio of 8, which corresponds to the highest step height in the present tests the effect can be expected to be perceptible but not serious. Approximately 85% of the data in this investigation were obtained at aspect ratios of 13.3 or greater where no aspect ratio effects are anticipated. Finally, one might expect that for the lower step-height to boundary-layer-thickness ratios of the present tests relative to those of Ref. 3 the end effects may appear at slightly higher aspect ratios than discussed here. Later in the paper it will become apparent that the deficiency in two-dimensionality for the highest step height in this investigation is much less serious than some of the deficiencies that will become apparent for some of the other data presented in this report.

Scaling Considerations

To determine the range of nondimensional parameters that may be pertinent to the analysis of the experimental pressure distributions, a dimensional analysis was made. The simplest combination of independent and dependent variables, compatible with two-dimensional flow with no heat transfer or stream pressure gradients, was chosen for the study. The dependent variables were the static pressure p and orifice location x. Among the independent variables, freestream conditions were represented by p_∞, ρ_∞, u_∞, μ_∞, and a_∞; the boundary-layer characteristics by the two variables δ^* and θ; and the step height by k. A large number of nondimensional combinations or parameters were found available for analysis. For this presentation, the choice was made to scale the static pressures p by the freestream static pressure p_∞, the orifice locations x by the step height k, and the step height k by the boundary-layer displacement thickness δ^*. For correlation purposes, the Reynolds number is specified in terms of δ^*. One should not infer by this choice that they are the only significant nondimensional parameters or even the best ones.

Pressure Distributions

Some typical results for the wall pressures ahead of the step determined in this investigation are presented in Fig. 3. The results are for $M_\infty = 1.61$ and $R_\delta{}^* = 2.54 \times 10^5$ only. Actually, similar data were obtained at two Mach numbers and at seven Reynolds numbers at each Mach number. A dimensional plot is utilized because all simple methods of normalization result in curves that cross over one another and obscure many significant details in plots where the step height k is a parameter.

For the largest step heights, as one approaches the step face from a distance, the pressure ratio p/p_∞ increases rapidly to a peak, decreases moderately to a trough, rises sharply to a second peak, and then decreases slightly just ahead of the step face. The initial portion of the pressure distribution is concave downward and appears to have a knee or region of smaller radius of curvature imbedded in the forward part. At the

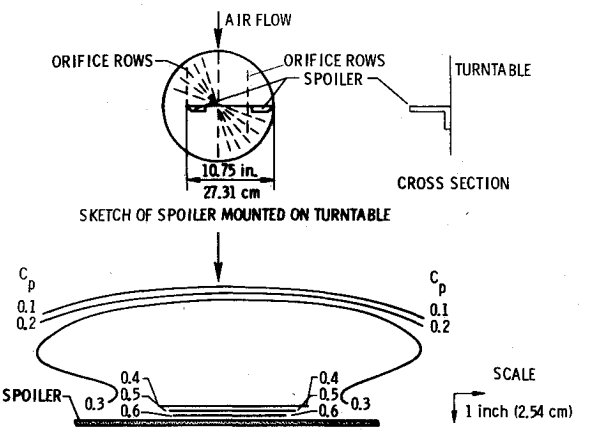

Fig. 2 Contour plots showing lines of constant-pressure coefficient in flowfield ahead of a spoiler. Reference 3, configuration 8, aspect ratio 12, $M_\infty = 1.61$, unit Reynolds number $= 1.2 \times 10^7$ per meter.

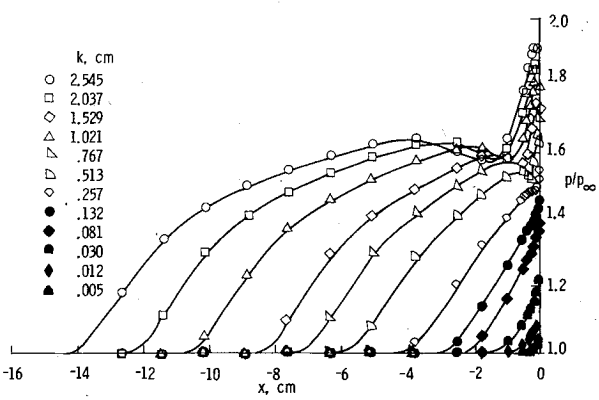

Fig. 3 Typical pressure distributions on wall ahead of forward-facing step. $M_\infty = 1.61$, $R_\delta{}^* = 2.54 \times 10^5$

smallest step heights, the pressure ratio increases monotonically and is concave upward. The general level of pressures is also much lower than for the higher step heights. For step heights in between there is a gradual transition from one type of pressure distribution to the other. The combination of large changes in pressure level and substantial changes in distribution shapes indicates that it will be a formidable problem to correlate the data in this regime of step-height to boundary-layer-thickness ratios (from nearly 0 to approximately 0.3). In most other experimental investigations the lowest step-height to boundary-layer-thickness ratios correspond to the largest ones investigated here; consequently, the lower range of ratios has been virtually neglected by other researchers.

A typical effect of Reynolds number on the pressure distribution is illustrated in Fig. 4. In this plot the abscissa has been nondimensionalized by the step height, and the scales have been shifted vertically relative to one another to eliminate undesirable overlapping. Two features readily stand out: one, the relatively large effect of Reynolds number; the other, the large increase in relative upstream influence as the step-height to boundary-layer-thickness ratio is decreased. The Reynolds number range of these tests is very large and at the lowest values the test section Mach number drops slightly and there occurs a combined Reynolds number and Mach number effect. Detailed studies indicate that this Mach number effect is discernible only at the two lowest Reynolds numbers and that elimination of this effect in the worst case will tilt upward the lowest curve (circular symbols) by about the size of the symbol at the first peak and less than two symbol heights at the second pressure peak. Obviously, the Reynolds number effect is too large to be discounted as has been done in some previous correlation studies.[4 and 5] In particular, one should not expect low Reynolds number data to correlate with high Reynolds number results.

Another interesting feature revealed in this plot is the tendency of the pressure distributions at a constant step height to cross one another at the same value of x/k. This tendency was found to hold for nearly all the data obtained in this investigation. A possible explanation is that the boundary-layer separation point lies in this region and moves only slightly with changes in $R_\delta{}^*$. (See also Figs. 12 and 15 of Ref. 6.) The height of the subsonic flow in the boundary layer at the separation point can be considered as a gate or valve through which pressure disturbances in the separated-flow region can propagate upstream and affect pressures in the nonseparated region. As $R_\delta{}^*$ decreases because of decreases in tunnel stagnation pressure, the boundary layer actually increases in thickness, the gate or valve opens wider, and upstream influence of the spearated-flow region increases in magnitude. The consequence of this interaction is an increase in pressure ahead of the separation point and a relief or decrease in pressures behind it. This relation of step height to subsonic flow height at the separation point also explains the large increase in relative upstream influence as the step height is decreased while $R_\delta{}^*$ is held constant. Note that the expected effects will be reversed if $R_\delta{}^*$ is decreased by decreasing the length of the boundary-layer run and thus also decreasing δ^*. To take into account the possibility of this reversed effectiveness, any general analysis of Reynolds number effects requires that the method of changing $R_\delta{}^*$ be specified, and that the two methods are not arbitrarily mixed.

Finally, from studies made at constant values of k/δ^* (specification of k being constant is generally insufficient), it was found that for the larger step heights which experience dips or troughs in pressure distribution, increasing $R_\delta{}^*$ tends to decrease the magnitude of the trough. The magnitude of the trough thus appears to be directly related to the shear existing in the boundary layer in the vicinity of the step face, decreasing as the local skin friction decreases.

The effect of Mach number on the pressure distributions is presented as Fig. 5. Fortunately, data at Mach numbers

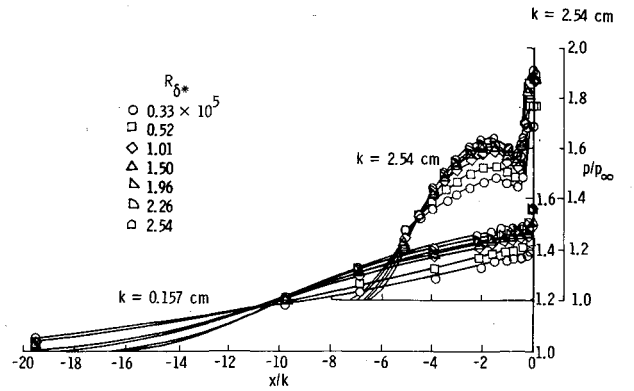

Fig. 4 Effect of $R_\delta{}^*$ on the two basic types of pressure distributions. $M_\infty = 1.61$.

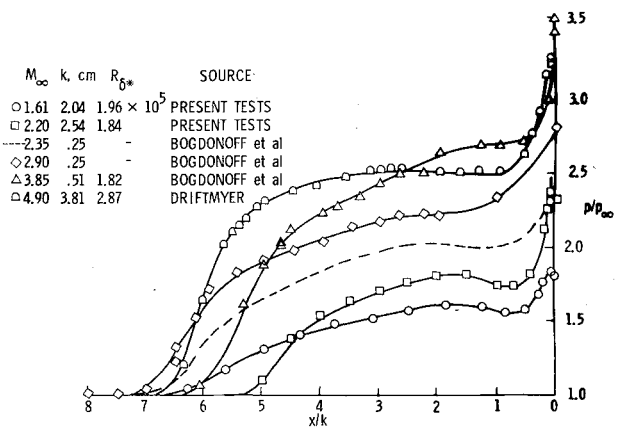

Fig. 5 Effect of M_∞ on pressure distributions. $k/\delta^* \approx 2$, $R_\delta{}^*$ as close to 1.82×10^6 as data permit.

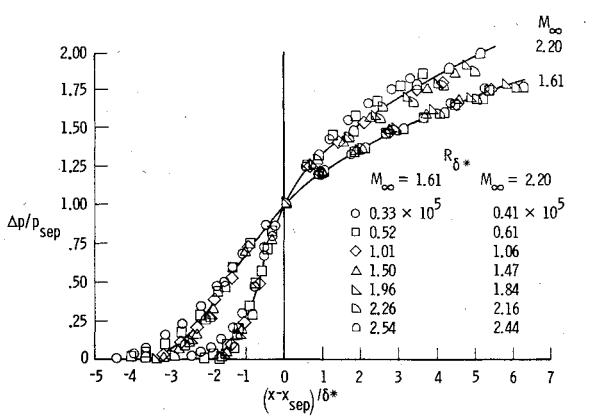

Fig. 6 Correlation of initial pressure rises for present results. $k = 2.54$ cm.

higher than those of the present investigation but at comparable step-height to boundary-layer conditions[5-9] were available to extend the comparison and enhance the probability of making useful conclusions. For all tests the ratio k/δ^* was approximately 2. The $R_\delta{}^*$'s for the Mach number 2.35 and 2.90 tests of Bogdonoff are not known, but because all tests were made in the same facility the presumption is made that the $R_\delta{}^*$'s for the lower Mach numbers are not excessively out of line with the value of 1.82×10^5 specified for the Mach number 3.85 tests. Matching of the Driftmyer[9] results with the other data in both k/δ^* and $R_\delta{}^*$ was not directly possible. The dashed line without symbols indicates that the individual pressures were not available in the report used to obtain the curve.[6]

In general, the shapes of the pressure distributions are basically similar except for the increasing level of pressure

with increasing Mach number. Changing the normalization of the pressures from the ratio form p/p_∞ to the usual pressure coefficient form $C_P=(p-p_\infty)/q_\infty$ tends to invert the relationships of the curves but does not result in any substantial improvement in correlation. Except for $M_\infty=2.20$ data of the present investigation, all pressure rises tend to initiate in the region of x/k between 6 and 7.5. This observation is made with reservations inasmuch as the data of Refs. 6-8 were obtained with a single static orifice fixed in the tunnel wall, with the step being moved relative to the orifice to obtain the pressure distributions. In view of the very high unit Reynolds number of the tests (95 million/m)[8] and thus an apparently short distance to the virtual origin of the tunnel-wall boundary layer, movement of the step may introduce a fortuitous Reynolds number effect which can make the complete comparison invalid. There also appears to be some deviatory behavior in the $M_\infty=3.85$ results relative to the others obtained in the same facility for which no explanation can be offered. As M_∞ is increased there is a general tendency for the trough in the pressure distributions to weaken and ultimately disappear. This trend again appears to be directly related to the shear in the boundary layer which decreases as M_∞ increases.

Correlation of Initial Pressure Rises

Some results of an attempt to correlate the initial pressure rises for the larger steps where the pressure distributions show evidence of troughs are shown in Fig. 6. The results are specified as applying to $k=2.54$ cm only. Actually, the correlations ahead of the separation point apply to any step height and the portions of the plots behind the separation point rotate slightly upward with decreasing step height but without any substantial change in character. The correlation was derived from the concept that, at constant $R_\delta{}^*$, changes in step height will not influence the pressure distributions upstream of the separation point.[10] With this assumption as a guideline, the pressure distribution curves for the lower step heights were shifted until they were coincident with the curve for $k=2.54$ cm and the after portions of the curves varied consistently with step height. The point where this transition from a single to multiple curves occurred at each $R_\delta{}^*$ was taken to be the separation point. The separation point locations and the separation pressure ratios indicated by this method were then backtracked and compared with those derived from the curve-crossover method previously discussed, and the agreement was found to be excellent. The curves were then renormalized in terms of the pressure at the separation point and the distance from the separation point normalized by δ^* and the results plotted as shown here. The symbols do not represent experimental pressure points but actually uniformly spaced points from the faired curves being correlated. This procedure saved time in computations, and use of symbols in the plots instead of line codes simplifies identification of the various $R_\delta{}^*$ curves.

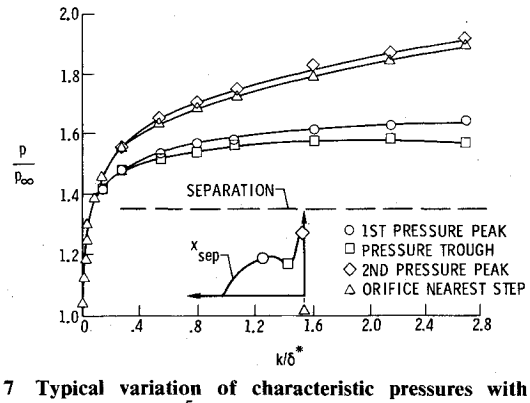

Fig. 7 Typical variation of characteristic pressures with k/δ^*. $M=1.61$, $R_\delta{}^*=2.54\times10^5$, $\delta^*=0.96$ cm.

The plots indicate that the correlations are reasonably good. With the use of an empirical correction factor based on the nondimensional height ratio $k/k_{2.54}$ the effects of step height can be added to provide a truly universal distribution for the initial pressure rise for each Mach number. Furthermore, Driftmyer finds a similar correlation at $M_\infty=4.90$ (Ref. 9, Fig. 13) and a preliminary examination of the Vas, Bogdonoff, Kepler results[6-8] indicates that this approach will be valid for these data also. Thus, the basic concepts from which the correlations were derived appear to be validated. Note, however, that δ^* is apparently only a first-order correlation factor for the pressure distributions ahead of the separation point; the true interpretation must be more complex.

Pressure Peaks, Troughs, and Other Similar Parameters

At this point, attention is turned from the study of pressure distributions as entities to a study of specific components of the distributions such as pressure peaks and troughs, separation pressure ratios, and other similar parameters. Toward this end, Fig. 7 presents some typical variations in such pressures with step height. The results are for a single Mach number, 1.61, and single $R_\delta{}^*$, 2.54×10^5. Four pressure parameters are plotted: the first pressure peak, the pressure trough, the second pressure peak, and the pressure at the orifice nearest the step face. The dashed line represents the separation pressures determined from the aforementioned correlation study for the larger step heights (defined at Type I separation).

Generally, only the first pressure peak is discussed in the literature, yet the other parameters can make significant contributions to the understanding of the boundary-layer separation phenomena being studied. Fox example, as will be shown later, it is believed that the troughs in pressure are generated by the existence of transverse vortices embedded in the separated-flow region. Consequently, the differences in pressure between the first peak and trough, and between the second peak and the last orifice, provide a rough estimate as to the strengths of these vortices. The data show that both vortices weaken gradually and disappear at about the same time, as k/δ^* is decreased. Also, the second pressure peak serves as a lower bound for estimating the maximum energy level within the separated flow region and thus provides a valuable clue as to one of the most significant characteristics of the dividing streamline. Finally, k is the only independent variable which varied in this plot, and it should be obvious from the shapes of the curves that no further refinement in correlation or understanding of the phenomena can be made without more detailed information on the boundary layer. In particular, for the lowest step heights, these pressures should be dependent upon the characteristics of only that part of the boundary layer close to the wall.

In Fig. 8 the pressure ratios for the first peak have been isolated from the others and plotted as a function of k/δ^* with $R_\delta{}^*$ as a parameter. Similar plots can be made for the other pressures and for the other test Mach number, but the general trends and conclusions will be nearly the same. The most significant conclusion to be derived from this figure is that, even at a constant value of k/δ^*, changes in $R_\delta{}^*$ have a significant effect on the levels of the curves. This suggests that the changes in velocity and density profiles that accompany the changes in $R_\delta{}^*$ are significant parameters in the problem of turbulent boundary-layer separation due to a forward-facing step and emphasize the previous statement that low and high Reynolds number data should not be arbitrarily correlated.

The variation of both the first peak and trough pressures with k/δ^*, with Mach number as a parameter, is presented in Fig. 9. The $R_\delta{}^*$'s for the results of the present investigation were chosen to correspond as closely as possible to that specified for the Bogdonoff tests at $M_\infty=3.85$. For the

Bogdonoff tests at $M_\infty = 2.35$ and 2.90 data, the $R_\delta{}^*$ values were not specified and had to be crudely estimated. To make the estimates, the ratio of δ^*/δ recorded for the $M_\infty = 3.85$ tests was used to determine which power velocity profile the data corresponded to in Ref. 11, and then this power and the given thicknesses δ were used to determine the δ^* values corresponding to the appropriate Mach numbers in the same tables. Nothing could be done without undesirable interpolation to bring the Driftmyer results to the desired value of $R_\delta{}^*$.

In general, at the lower values of k/δ^*, all data show the same trend, an increase in the pressure ratios p/p_∞ with increasing k/δ^*. At the higher values of k/δ^*, the Bogdonoff data indicate a trend toward peaking, with the peaks in the curves occurring at progressively lower values of k/δ^* as M_∞ is increased. A comparison of the present $M_\infty = 1.61$ data with some spoiler tests made at the same Mach number in the same facility at lower values of $R_\delta{}^*$ but higher k/δ^*[3] reveal that this peaking trend may not be valid. The tests of Driftmyer were not extended to sufficiently high values of k/δ^* to make any contributions toward confirming or denying this tendency toward peaking. There is a possibility that the peaking in the Bogdonoff data may be caused by the method of making the tests. As k was increased it was necessary to move the step back from the orifice to register the peak in pressure. Rearward step movement causes an increase in effective $R_\delta{}^*$ and a decrease in k/δ^*, each having a different effect on the peak pressure. A possibility exists that each effect may be dominant in different ranges of k/δ^*. The reason for the apparent change in trend with Mach number indicated by the $M_\infty = 3.85$ and 4.90 results is not known, but in the discussion of Fig. 5 the $M_\infty = 3.85$ data were mentioned as being suspect.

A somewhat different approach is utilized to assess the effects of Mach number in Fig. 10. Here the pressures are plotted as functions of Mach number with the various pressures as parameters. The figure is essentially a cross plot of the previous figure at $k/\delta^* \approx 2$, the only value near which data for all Mach numbers are available. Included in the figure is a curve due to Bogdonoff[7] for the pressure required for an incident shock to separate a turbulent boundary layer.

The main conclusion to be derived from this figure is that the shapes, and to some extent, levels of the curves are heavily dependent upon the $M_\infty = 3.85$ and $M_\infty = 4.90$ data which have been shown previously to have some disagreement between each other. Obviously, more data of good quality are needed to establish the proper trends.

Peak, Trough, and Boundary-Layer Separation Distances

The variation of the peak, trough, and separation distances (separation distances were found by the method discussed in Fig. 4) with k/δ^* as determined in the present investigation are illustrated in Fig. 11 for $M_\infty = 1.61$. Similar trends were found at $M_\infty = 2.20$. Except for the case of the separation distances, the results tend to coalesce into single curves for each characteristic distance. This signifies that the effect of $R_\delta{}^*$ on these distances in relatively weak. Even the estimated separation distance data appear to coalesce into a single curve at high values of k/δ^*.

The estimated separation distances decrease with increases in k/δ^*. The distances to the bottom of the trough and to the top of the first peak, on the other hand, increase with k/δ^*, at first rapidly and then rather slowly. Above a k/δ^* of about 0.3 or 0.4 the increases in the trough and first peak distances are essentially directly proportional to each other. The slight decrease in x/k indicated for the second pressure peak with increasing k/δ^* may be due to a bias resulting from the small number of orifices used to locate the peak.

The variation in first peak and trough distances with k/δ^* with Mach number as a parameter is presented in Fig. 12.

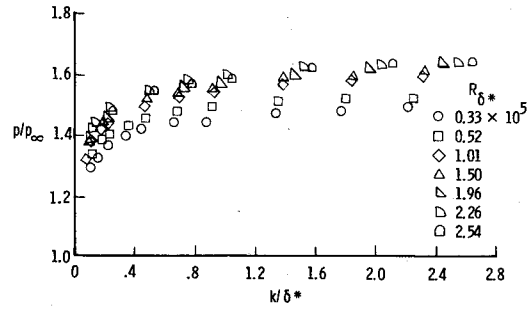

Fig. 8 Effect of k/δ^* on first peak pressures with $R_\delta{}^*$ as parameter. $M_\infty = 1.61$.

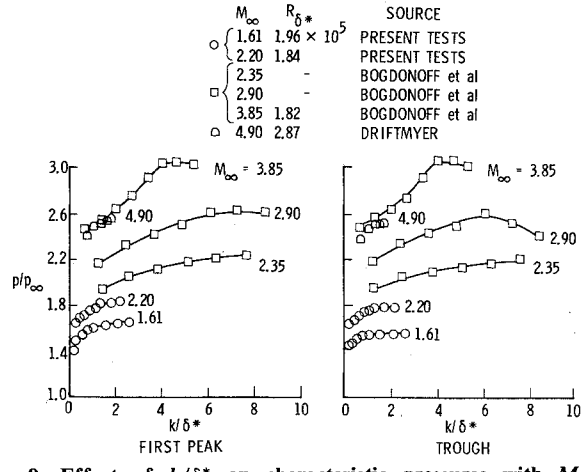

Fig. 9 Effect of k/δ^* on characteristic pressures with M_∞ as parameter. $R_\delta{}^*$ as close to 1.82×10^5 as data permit.

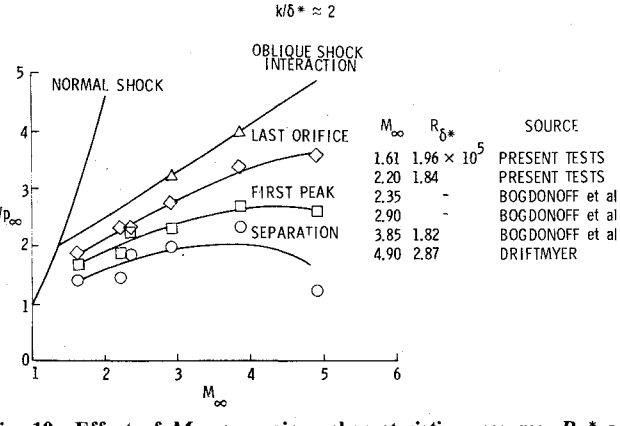

Fig. 10 Effect of M_∞ on various characteristic pressures. $R_\delta{}^*$ as close to 1.82×10^5 as data permit.

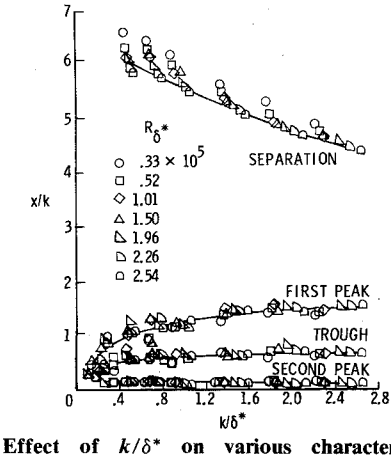

Fig. 11 Effect of k/δ^* on various characteristic distances. $M_\infty = 1.61$.

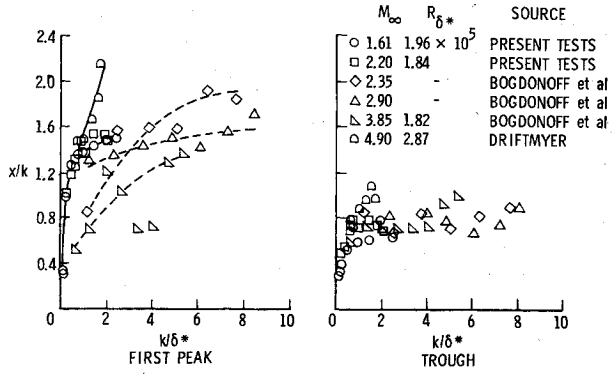

Fig. 12 Effect of k/δ^* on various characteristic distances with M_∞ as parameter.

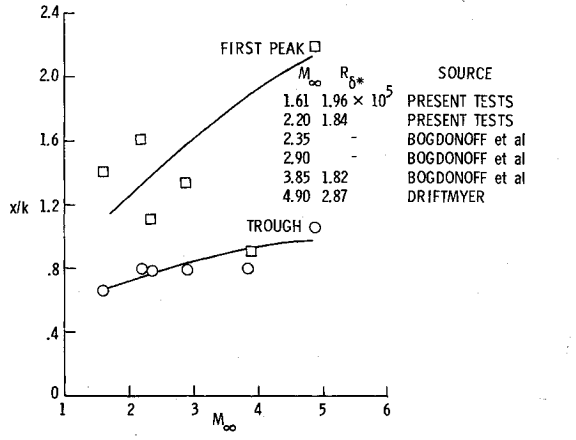

Fig. 13 Effect of M_∞ on various characteristic distances. $k/\delta^* \approx 2$.

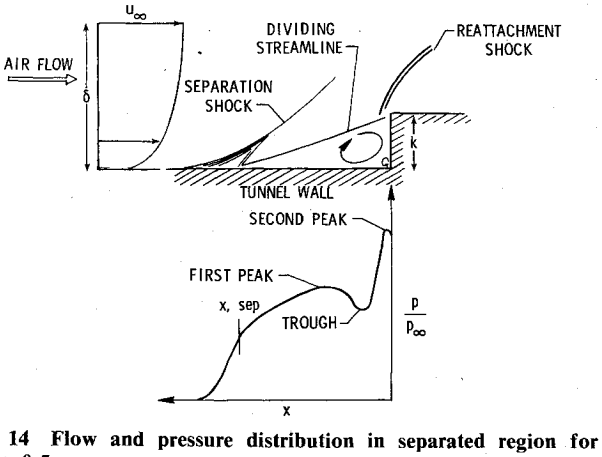

Fig. 14 Flow and pressure distribution in separated region for $k/\delta^* > 0.5$.

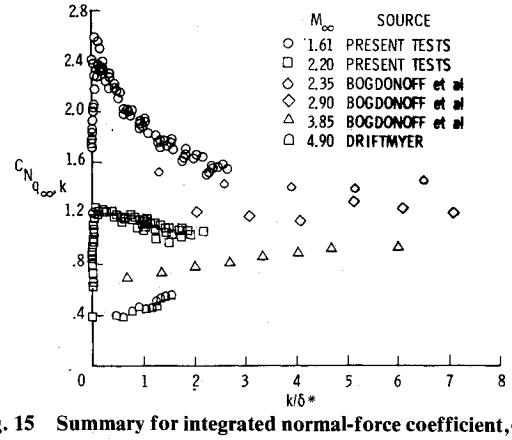

Fig. 15 Summary for integrated normal-force coefficient, C_N.

Again the data for the different Mach numbers are matched as well as possible in terms of $R_\delta{}^*$. There is a considerable amount of scatter, particularly in the data for the first pressure peak. A part of the scatter derives from the relative flatness of the peaks in many cases, but in some instances the peak and trough areas have not been sufficiently well defined by judicious location of the static-pressure orifices. The data indicate that both the peak and trough distances increase with k/δ^* at the lower values of k/δ^* and then tend to approach a common value at all Mach numbers except for the $M_\infty = 4.90$ tests. These common values are about 1.6 for the peak-pressure distance and 0.8 for the trough distance, or in a ratio of approximately 2 to 1. Although not shown, the separation distances show even larger anonalies and possible discrepancies than these data, indicating that the methods of determining separation could stand some improvement.

The effects of Mach number on the peak and trough distances are presented in another form in Fig. 13. Here the distances have been plotted as direct functions of M_∞. Obviously, the scatter is too great to provide any meaningful conclusions. Inasmuch as accurate location of pressure peaks and troughs is essential to the development of theoretical and empirical methods for estimating the complete distributions and understanding the basic interaction phenomena, it would appear desirable to be able to track them more accurately.

Deduced Flow Model

From an analysis of the types of pressure distributions presented in this paper and from schlieren photographs which have not been discussed here, the phenomenological model illustrated in Fig. 14 is deduced. This model applies to the higher step heights where the first pressure peak and trough are discernible. Except for the secondary vortex in the corner, the model is identical to that identified by most researchers.

The boundary layer separates from the surface at the point marked x, sep. Because of upstream pressure propagation through the subsonic part of the boundary layer, the actual pressure rise at the surface begins some distance ahead of the separation point. Downstream of the separation point is a region of recirculating air separated from the exterior boundary-layer flow by a separation or dividing streamline. This streamline reattaches to the step face somewhere below the corner. The exact shape of the dividing streamline is not known because of too few flowfield measurements and because the streamline lies near a region of nearly maximum turbulence production which masks the curvature of the local flow in schlieren photographs. If the streamline is concave upward to a sufficient degree Goertler vortices[12] may be generated in the turbulent boundary layer which could complicate even more the difficult task of developing theoretical methods for computing the flow. Embedded within the separated-flow region parallel to the step face is a large vortex. There is also some evidence of a very much smaller counterrotating vortex beneath the main one. For a constant k/δ^* the vortex tends to weaken as the Reynolds number or Mach number is increased. As the step height is decreased the peaks and troughs disappear and the pressure increases monotonically from the boundary-layer separation point to the step face. Too little is known about the separated-flow region in this case to justify speculation. Note that the flow characteristics downstream of the step face have not been identified in the flow model because the downstream pressure distributions made in the present tests have not yet been analyzed.

Integrated Normal-Force Coefficients

A measure of the normal force required to deflect the boundary layer so it can accomplish its passage over the step is provided by the integrated normal-force coefficient. To illustrate the characteristics of this normal force, the normal-force coefficients for all the results of the present investigation, and those of Vas, Bogdonoff, and Kepler and

Driftmyer are presented in Fig. 15. In the low k/δ^* range ($k/\delta^* < 3$ or 4) there is a very large effect of Mach number. As k/δ^* is increased toward the maximum test values, the results for the different Mach numbers tend toward a broad but common region centered around a C_N of about 1.2. As k/δ^* is decreased from 3 or 4, the lower Mach number data show a rise in the normal-force coefficient, whereas the higher Mach number data ($M_\infty \geq 3$) show a decrease. The present results, which were extended to much lower values of k/δ^* than in the other investigations, peak at a $k/\delta^* \sim 0.1$ and then the normal-force coefficients drop precipitously with further decrease in k/δ^*. These decreasing normal-force coefficients are associated with the monotonically increasing, concave-upward pressure distributions previously described. The apparent scatter in the present results and Drifymyer's $M_\infty = 4.90$ data is due to Reynolds numbers effects which are not identified in this plot. The largest Reynolds number effects occur at the largest values of k/δ^* where the vortices in the separated-flow region are strongest. From the general trends in Mach number effects it would appear that the present results at $M_\infty = 2.20$ are too low. This anomaly, if it is one, arises from the fact that the initial pressure rise at $M_\infty = 2.20$ occurs closer to the step face than at the other Mach numbers as was noted in the discussion of Fig. 5. The normal-force coefficients for the present investigation were also computed using the mean dynamic pressure within that part of the unseparated boundary layer corresponding to the step height, but this approach actually decreased the tendency toward correlation of the overall results. The conclusion is that the normal-force coefficients are more closely related to free-stream conditions than to those within the boundary layer.

Conclusions

Pressure distribution tests were made at Mach numbers of 1.61 and 2.20, over a step-height range from 0.005 to 2.54 centimeters, and an effective length Reynolds number range from about 8 to 150 million. The results were compared with some obtained at higher Mach numbers at approximately comparable boundary-layer conditions. The comparison showed several unexplainable anomalies, and pointed up the lack of boundary-layer information necessary for a proper analysis. It also indicated a need for more tests over the full Mach number range to provide data for direct comparison over a wider range of pertinent parameters. Recommendations are made to more accurately define in future test the pressure distributions close to the step face and to present the full complement of the associated boundary-layer data, including velocity and density (or temperature) profiles. An analysis of the data also indicates the existence of a transverse vortex in the separated-flow region which weakens with increase in Reynolds and Mach numbers and significantly affects the pressure distributions.

References

[1] Czarnecki, K.R. and Monta, W. J., "Pressure Distributions and Wave Drag Due to Two-Dimensional Fabrication-Type Surface Roughness on an Ogive Cylinder at Mach Numbers 1.61 and 2.01," NASA TN D-835 June 1961.

[2] Jackson, M.W., Czarnecki, K.R., and Monta, W.J., "Turbulent Skin Friction at High Reynolds Numbers and Low Supersonic Velocities," NASA, TN D-2687, March 1965.

[3] Lord, D.R. and Czarnecki, K.R., "Aerodynamic Loadings Associated With Swept and Unswept Spoilers on a Flat Plate at Mach Numbers of 1.61 and 2.01" NACA RM L55L12, Nov. 1955.

[4] Zukoski, E.E., "Turbulent Boundary-Layer Separation in Front of a Forward-Facing Step," *AIAA Journal*, Vol. 5, Oct. 1967, pp. 1746-1753.

[5] Sterrett, J.R. and Emery, J.C., "Extension of Boundary-Layer Separation Criteria to a Mach Number of 6.5 by Utilizing Flat Plates With Forward-Facing Steps," NASA, TN D-7453, 1960.

[6] Vas, I.E. and Bogdonoff, S.M., "Interaction of a Turbulent Boundary Layer With a Step at $M = 3.85$," AFOSR TN 55-200, April 1955, Air Force Office of Scientific Research, Arlington, Va.

[7] Bogdonoff, S. M., "Some Experimental Studies of the Separation of Supersonic Turbulent Boundary Layers," Princeton University Report 336, June 1955, Princeton, N.J.

[8] Bogdonoff, S.M. and Kepler, E. C., "The Separation of a Supersonic Turbulent Boundary Layer," Institute of the Aeronautical Sciences 22nd Annual Meeting, New York N.Y., Preprint 441, June 1954.

[9] Driftmyer, R.T., "A Forward Facing Step Study: The Height Less Than the Boundary-Layer Thickness," NOLTR 73-98, May 1973, Naval Ordnance Lab., White Oak, Silver Spring, Md.

[10] Chapman, D.R., Kuehn, D.M., and Larson, H.K., "Investigation of Separated Flows in Supersonic and Subsonic Streams With Emphasis on the Effect of Transition," NACA, Rep. 1356, 1958.

[11] Tucker, M., "Approximate Calculation of Turbulent Boundary-Layer Development in Compressible Flow", NACA, TN 2337, April 1951.

[12] Goertler, H., "Über eine dreidimensionale Instabilität laminarer Grenzschichten an konkaven Wänden," Ges. d. Wiss. Göttingen, Nachr. a. d. Math., Bd. 2, Nr. 1 1940, trans. NACA Technical Memorandum 1375, 1954.